

SRM Based PV System for Irrigation Pumps

K Vijaya Sagar, T Jnana Prasannamba

Department of EEE, Godavari Institute of Engineering & Technology (A), Rajahmundry, Andhra Pradesh, India.

Abstract : This project investigates the design of a cost-effective and efficient solar powered irrigation pump utilizing a switched reluctance motor (SRM). It utilizes a simple DC-DC boost converter as a power conditioning stage between SPV array and the motor drive. The control of solar photovoltaic (SPV) array output power at maximum power point (MPP) and facilitating the soft-starting to the SRM drive, are two prime functions of the boost converter. The use of a 4-phase SRM drive minimizes the torque ripple and increases the number of strokes without incrementing the number of rotor poles. The low number of switches in a mid-point converter used to energize SRM phases further enhances the performance of the system. The speed control of the motor using the pulse width modulation (PWM) switching of split capacitor converter eliminates the requirement of additional sensors on the motor to control its speed. The proposed water pumping system is designed, modeled and its performance is simulated on MATLAB/Simulink platform and its responses are analyzed, under the varying environmental conditions, which authenticate its appropriateness as an irrigation pump.

I. INTRODUCTION

Solar Photovoltaic (PV) is a key technology option to realize the shift to a decarbonised energy supply and is projected to emerge as an attractive alternative electricity source in the future. Globally, the solar PV grid connected capacity has increased from 9.4 GW in 2007 to 15.7 GW in 2008 and was 67.4 GW at the end of 2012. Nowadays it is necessary to reduce the costs and increase the efficiency to make solar energy to be more useful. As a result, many research works address the development of solar power system in recent years with improved performances. Power electronics is a green technology, converting electrical energy from one form to another, achieving high conversion efficiency of the solar PV-powered system. The efficiency of solar PV powered-system depends mainly on the efficiency of the Maximum Power Point Tracking (MPPT) circuits.

II. PHOTOVOLTAIC ENERGY SYSTEM

The output of solar PV cell is a Direct Current (DC), where the current is determined by the area of the cell and amount of exposed solar irradiation. The voltage of the individual silicon cell is in the order of 0.5V. Thereby, the cell has to be connected in a series to constitute modules with reasonable voltage level. The maximum power is delivered at the operating point, where the magnitudes of PV system and load resistance are equal. This is usually performed by an interfacing DC-DC power converter employing certain MPPT technique and algorithm. The operating point is held at MPP by regulating either the current or voltage of the MPPT converter.

PV systems are usually used in three main fields: 1. Satellite applications, where the solar arrays provide power to satellites, 2. Off-grid applications, where solar arrays are used to power remote loads that are not connected to the electric grid, and 3. On-grid, or grid connected applications, in which solar arrays are used to supply energy to local loads as well as to the electric grid.

The basic element of the solar PV power conditioning system is the DC-DC converter. If the purpose is to charge a battery or regulate a DC- bus as in space and telecom applications, the system can be implemented by using only the DC-DC converter as depicted

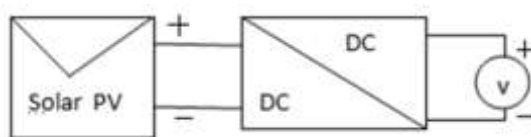


Figure 1.1: Basic element of power conditioning system

III. POWER CONVERTERS IN PV SYSTEM

Photovoltaic system is gaining increased importance as a renewable source because of its advantages such as the absence of fuel cost, little maintenance and no noise and wear due to the absence of moving parts. But there are still two principal barriers to the use of photovoltaic systems: the high installation cost and the low energy conversion efficiency.

A PV panel is a non-linear power source, i.e., its output current and voltage (power) depend on the terminal operating point. The maximum power generated by the PV panel changes with the intensity of the solar radiation and the operating temperature. To increase the ratio of output power/cost of the installation, the PV panel should operate in the maximum output power point.

Characteristics of Solar PV Module

Solar cells consist of a p-n junction fabricated in a thin layer of semiconductor. The semiconductor electron can be located in either the valence band or conduction band. Initially, all the electrons in the semiconductor fill up the valence band but when sunlight hits the semiconductor, some electrons acquire enough energy to move from the valence band to the conduction band. The electrons in the conduction band, then, begin to move freely creating electricity. The electron leaving the valence band leaves a positively charged hole behind and now the valence band is no longer full; it aids the current flow. Most solar cells are doped to reduce the energy required for the electron to move from the valence band to the conduction band.

The amount of energy from sunlight that is absorbed by a solar cell determines its efficiency. This energy is called photon and it can be reflected, absorbed or it can pass through a semiconductor. Since only the photons that are absorbed contribute to the electrical energy, it is important to reduce the percentage of photons that pass through and are reflected. An anti-reflective coating is usually applied to the surface of the solar cell to decrease the number of photons that are reflected. This reduces the percentage of photons reflected but some photons are still able to pass right through the semiconductor material.

There are several approaches to manufacturing solar cells, including the kind of semiconductor used and the crystal structure employed, with each different factor affecting the efficiency and cost of the cell. Other external factors such as the ambient weather conditions like temperature, illumination, shading, etc., also affect the solar panel’s output. The aim is to design a system that will extract the most possible power regardless of ambient weather conditions or solar cell efficiency.

Modeling of Solar PV Module

A simplified equivalent circuit of a solar cell consists of a diode and a current source which are switched in parallel. The photocurrent generated when the sunlight hits the solar panels can be represented with a current source and the p-n transition area of the solar cell can be represented with a diode. The voltage and current relationship of the simplified solar cell can be derived from Kirchhoff’s current law. This simplified equivalent circuit, however, does not give an accurate representation of the electrical process at the solar cell. On real solar cells, voltage losses occur at the boundary and external contacts and leakage currents occur throughout the cell; these losses can be represented with a series resistance R_s and a parallel resistance R_p , respectively. The equivalent circuit of the solar cell showing the series and parallel resistance is shown in Figure 2.4

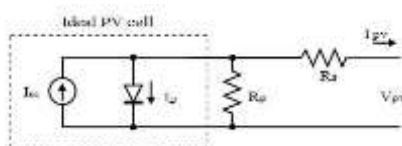


Figure 2: Equivalent circuit of a solar PV module

For Figure.2 the current equation is given by

$$I_{sc} = I_D + I_{pv} + (V_D / R_p) \tag{2.1}$$

$$V_{pv} = V_D - (I_{pv} * R_s) \tag{2.2}$$

where diode current is $I_D = I_o + (e (V_D / V_t) - 1)$, I_{sc} is the short circuit current, $V_t = N_s K T / q$ is the thermal voltage with N_s cells connected in a series (K is the Boltzmann constant, q is the electron charge and T is the temperature of the PV cells). The short circuit current is directly proportional to the irradiation and slightly proportional to the level of the cell temperature.

Using Equations 2.1 and 2.2, the solar PV module is modeled in MATLAB/Simulink as shown in Figure 2.4 and used to enhance the understanding and predict the I-V and P-V characteristics and to analyze the effect of temperature and irradiation variation. If irradiance increases, the fluctuation of the open-circuit voltage is very small. But the short circuit current has sharp fluctuations with respect to irradiance. However, for a rising operating temperature, the open-circuit voltage is decreased in a non-linear fashion.

The P-V and I-V characteristics are validated in MATLAB software for the L1235-37Wp (Watt peak) solar module. Table 2.1 shows the technical specification of L1235-37Wp solar panel under test which is shown in Figure 2.5. The I-V characteristic is obtained based on experimental results under irradiation = 1000 W/m², temperature = 25°C.

Table 2.1 Specification of a solar PV module under test

Parameter	Values
Open circuit voltage (V_{oc})	21V
Short circuit current (I_{sc})	2.5A
Voltage at MPP (V_{max})	16.4V
Current at MPP (I_{max})	2.25A
Power rating (P_{max})	37W
Maximum system voltage	600V
Module efficiency (%)	10.82%
Size (mm)	645*530*16
Weight (kg)	4

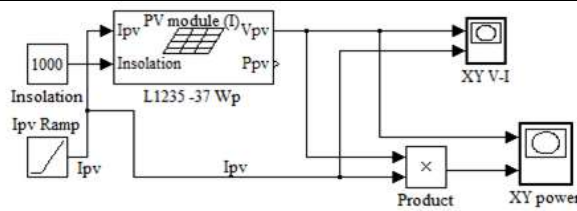


Figure 2.4: MATLAB model for PV module

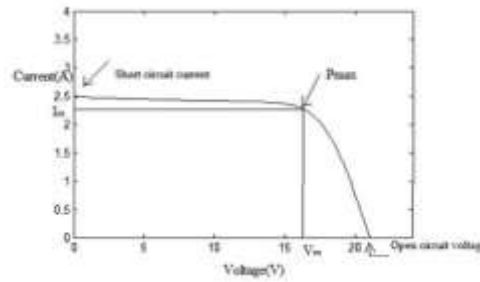


Figure 2.5: I-V Characteristics of solar PV module

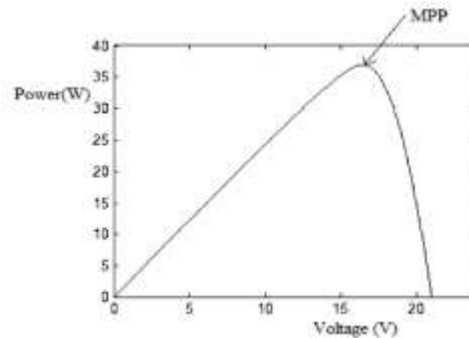


Figure 2.6: P-V Characteristics of solar PV module

IV. DC-DC CONVERTERS IN A SOLAR PV SYSTEM

PV interfacing is a challenging task and there is a need for clarification of the existing DC-DC converter topologies used in the PV applications. DC-DC converter shown in Figure 3.1 is an essential element in the MPPT process and this process can be performed either by controlling the input current or voltage of the interfacing converter. Also it is known that DC-DC converters increase or decrease the magnitude of the DC-voltage and/or invert its polarity. This is accomplished by the pulse width modulation technique, usually to a constant frequency. The duty cycle (d) is the ratio of the time of conduction (T_{ON}) to the switching period (T_s). The three basic configurations of converters (buck, boost and buck-boost derived) are similar to a DC transformer, both in continuous conduction mode (CCM) and discontinuous conduction mode (DCM). In a DC transformer, the relationship of transformation can be controlled electronically by changing the duty cycle of the converter from the range 0 to 1.

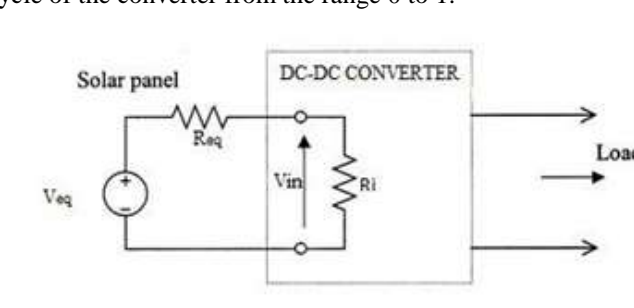


Figure 3.1: MPPT process using DC-DC converter

The power electronics interface is connected between a solar panel and a load or battery bus is a pulse width modulated DC-DC converter or their derived circuits operating in Discontinuous Inductor Current Mode (DICM) or Discontinuous Capacitor Voltage Mode (DCVM) is used to extract maximum power from solar PV panel. The DC-DC converter has the input resistance characteristics being proportional or inversely proportional to the switching frequency. Hence, by adjusting the nominal duty cycle of the main switch of DC-DC converter, the input resistance can be made equal to the equivalent output resistance of the solar PV panel and ensures the maximum power transfer.

V. PROPOSED SRM DRIVE CONVERTER

A. Converter Topology

Fig. (4) shows the per phase structure of the proposed SRMdrive topology. The converter operation is simple with a minimum number of switches while performing phase current commutation quickly. Regarding the number of switches used, the converter is similar to the R-dump converter, and it functions like the C-dump converter since the phase inductance energy is recovered. In fact, in addition to its simple structure, this converter has higher efficiency than the R-dump converter and a simpler structure and higher phase current commutation speed than the C-dump converter.

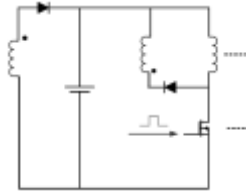
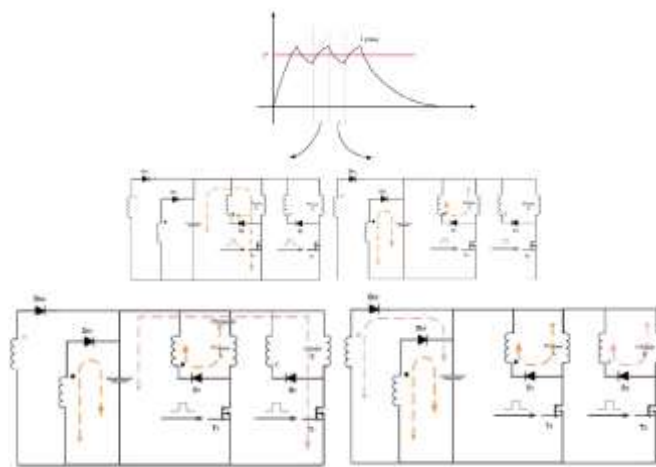


Fig. 4. Proposed SRM per phase converter

Fig. (5) shows the operating modes of this converter for 2 phase SRM. As shown in Fig. (5-a), in the magnetization mode, the switch T1 turns on in order to magnetize phase 'a'. As T1 turns on, the energy is transferred from the source to phase winding and the current in phase inductance increases. Also, in this mode if the magnetizing inductance of coupled inductors is not reset yet, diode D1 would conduct the magnetizing inductance current of the coupled inductors and the input voltage would reset this inductor. When the magnetizing inductance of coupled inductors is reset, Diode D1 turns off. The reset of coupled inductors magnetizing inductance is similar for other phases.

When the phase current reaches the reference, T1 is turned off and demagnetization starts. This mode is shown in Fig. (5-b). Since the voltage across phase winding is reversed, diode D1 turns on in this mode. When D1 turns on, D1 turns on and a negative voltage is placed across the phase winding in proportion to the coupling ratio which accelerates phase current commutation. Fig.(5-c) and Fig. (5-d) show two overlapping modes of stator phase currents. In the first mode, the phase inductance 'a' is being demagnetized and phase 'b' is being magnetized. In the second mode, both 'a' and 'b' phases are being demagnetized. As it can be observed, this converter has the ability to separately control phase currents. Also, It is important to notice that the snubber circuit of each switch will absorb the voltage spikes across the switches that otherwise would occur due to leakage inductance of coupled inductors.



(a) Magnetization mode (b) Demagnetization mode (c) Overlap of two phases: mode 1 (d) Overlap of two phases: mode 2

B. Design considerations

For designing this converter, the coupled inductors ratio has to be determined considering the performing speed of the drive. As shown in Fig. (1), if the phase current does not reach zero fast enough during the commutation, the phase current continues to exist in the negative torque production area and the phase torque becomes negative. This negative torque will cause large ripples in the torque generated by the motor. This is especially important at higher speeds, because higher speed requires faster commutation. So, each SRM drive can function to an extent of speed with regard to its converter's structure. The maximum SRM drive speed depends on the type of converter used and is illustrated by the following equation $T_f = \tau_a \ln \left[1 + \frac{R_s I_p}{V_c} \right]$ (1)

where T_f is the time needed for the current to reach from reference value to zero, τ_a is the electrical time constant of machine phases, R_s is the resistance of each phase winding, V_c is the reverse voltage applied to the phase inductance during commutation. The electrical time constant equation of the machine is as follows

$$\tau_a = \frac{L_a}{R_s} \quad (2)$$

As shown in Fig. (1), the phase inductance at the current commutation area equals to aligned inductance, thus L and τ would take an "a" subscript. Current drop angle at speed ω is shown as θ_f in Fig. (1) and is calculated as follows. $\theta_f = \omega_m T_f =$

$$[\omega_m \tau_a] \ln \left[1 + \frac{R_s I_p}{V_c} \right] \quad (3)$$

As it can be observed from (3), when speed increases, θ_f becomes larger resulting in a larger negative torque and, consequently, more torque ripples. Therefore, it is needed to look for a way to reduce θ_f at higher speeds. As it can be observed from (3), commutation can be carried out faster by increasing V_c . In the proposed converter, the reverse voltage across the phase winding can be increased for faster commutation purposes by increasing the coupled inductors L_1 and L_2 turns ratio. Also it is important to notice that V_c is constant in most of the converters introduced so far. But, in this converter, V_c can be designed by changing the coupled inductors turns ratio considering the maximum SRM drive functioning speed.

VI. SIMULATION RESULTS

In this section, the simulation results of SRM drive using the proposed converter is compared to the results of a SRM drive that uses a regular asymmetric converter. The schematic of this converter is shown in Fig. 6.

For simulation purposes coupling ratio is selected 2.3. Figure 5.1 shows the SRM phase currents that are driven by a regular asymmetric converter at 1500 rpm. Figure (5.2) shows the phase currents of the same motor at 4000 rpm.

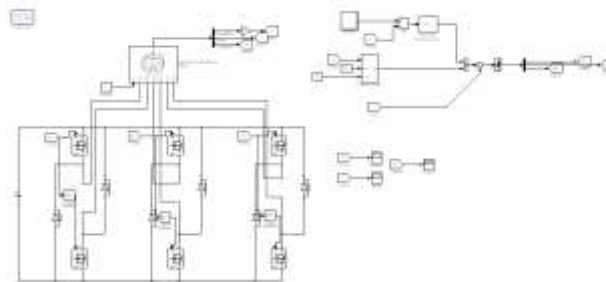


Fig 5.1 Simulink diagram of Asymmetric converter

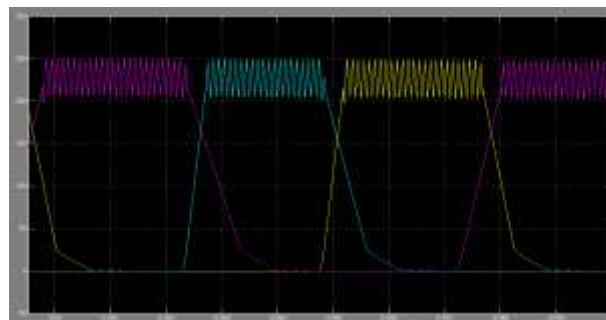


Fig: 5.2 Phase current waveforms of SRM driven by asymmetric converter at 1500 rpm asymmetric converter at 4000 rpm.

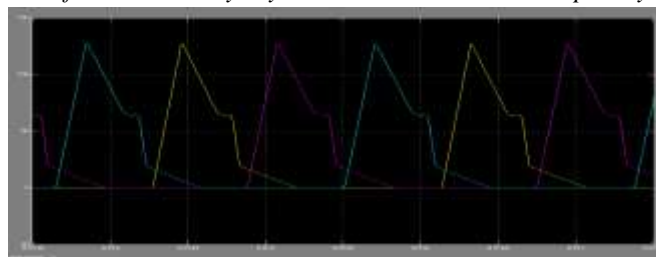


Fig 5.3 Phase current waveforms of SRM driven by asymmetric converter at 4000 rpm.

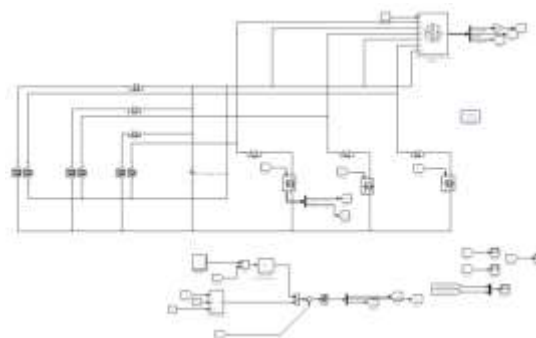


Fig 5.4 Simulink diagram of Proposed converter

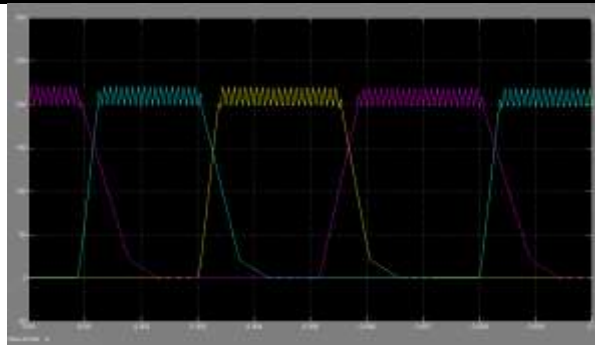


Fig 5.5 Phase current waveforms of SRM driven by proposed converter at 1500 rpm.

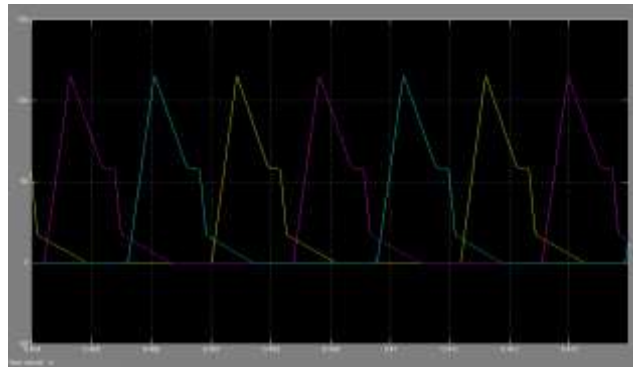


Fig 5.6 Phase current waveforms of SRM driven by proposed converter at 4000 rpm.

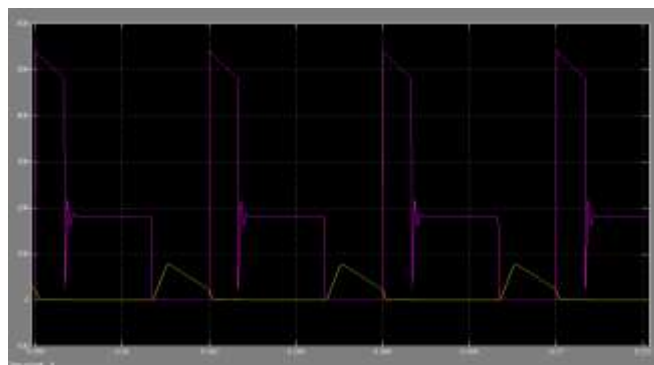


Fig 5.7 Voltage and current waveforms of one switch

VII. CONCLUSIONS

The design of a low cost PV powered SRM employed irrigation pump using a boost converter has been suggested and appropriateness of it has been demonstrated through examining its various responses in MATLAB/Simulink platform. A simple and efficient method for speed control of SR motor has been achieved, which provides the privilege for reduction of current sensors on the motor side. The PWM switching of a mid-point converter has been utilized which requires small rating split capacitors. The controlled starting of SR motor has been achieved using the perturbation size adjustment in the MPPT controller. The occasional self-start failure of 4-phase SR motor has been also acknowledged in proposed system and it has efficiently eliminated by implementing appropriate commutation angle dependent control. The overall behavior of proposed system even under rapidly changing environmental conditions concludes its suitability for PV based irrigation system.

REFERENCES

- [1] K. Hyung, H. Shin, J. I. Ha and A. Yoo, "Efficiency control of multistring PV system considering switching losses analysis," In Proc. Of IEEE Applied Power Electronics Conference and Exposition – APEC2014, Fort Worth, TX, 2014, pp. 3143-3149.
- [2] J. D. Bastidas-Rodriguez, E. Franco, G. Petrone, C. A. Ramos-Paja and G. Spagnuolo, "Maximum power point tracking architectures for photovoltaic systems in mismatching conditions: a review," IET Power Electronics, vol. 7, no. 6, pp. 1396-1413, June 2014.
- [3] X. Xiao, X. Huang and Q. Kang, "A Hill-Climbing-Method-Based Maximum-Power-Point-Tracking Strategy for Direct-Drive Wave Energy Converters," IEEE Transactions on Industrial Electronics, vol. 63, no. 1, pp. 257-267, Jan. 2016.
- [4] M. H. Uddin, M. A. Baig and M. Ali, "Comparison of 'perturb & observe' and 'incremental conductance', maximum power point tracking algorithms on real environmental conditions," in Proc. International Conference on Computing, Electronic and Electrical Engineering (ICE Cube), Quetta, Pakistan, 2016, pp. 313-317.
- [5] R. J. K. Prasana, S. Ramprasath and N. Vijayarathi, "Design and analysis of hybrid DC-DC boost converter in continuous conduction mode," in Proc. International Conference on Circuit, Power and Computing Technologies (ICCPCT), Nagercoil, 2016, pp. 1-5.
- [6] N. Chandrasekaran and K. Thyagarajah, "Modeling and performance study of single phase induction motor in PV fed pumping system using MATLAB," Int. J. Electr. Eng., vol. 5, no. 3, pp. 305-316, 2012.
- [7] R. Antonello, M. Carraro, A. Costabeber, F. Tinazzi and M. Zigliotto, "Energy-efficient autonomous solar water-pumping system for permanent magnet synchronous motors," IEEE Transactions on Industrial Electronics (Early Access).
- [8] H. Hembach, S.A. Evans and D. Gerling, "Systematic comparison of BLDC motors for small automotive water pump applications," in Proc. of 18th International Conference on Electrical Machines, ICEM2008, 6-9 Sept. 2008, pp. 1-5.
- [9] B. Singh and R. Kumar, "Simple brushless DC motor drive for solar photovoltaic array fed water pumping system," IET Power Electronics, vol. 9, no. 7, pp. 1487-1495, 6 8 2016.
- [10] J. H. R. Enslin and D. B. Snyman, "Combined low-cost, high-efficient inverter, peak power tracker and regulator for PV applications," IEEE Transactions on Power Electronics, vol. 6, no. 1, pp. 73-82, Jan 1991